THE JOURNAL OF PHYSICAL CHEMISTRY C
A JOURNAL OF THE AMERICAN CHEMICAL SOCIETY

pubs.acs.org/JPCC

Article

Structural Relaxation Rate and Aging in Amorphous Solids

Jiří Málek*

Cite This: J. Phys. Chem. C 2023, 127, 6080−6087

Read Online

ACCESS | Metrics & More | Article Recommendations

ABSTRACT: The structural relaxation in amorphous materials is discussed within the Tool−Narayanaswamy−Moynihan model (TNM), the Kovacs−Aklonis−Hutchinson−Ramos model (KAHR), and the entropy-based Adam−Gibbs−Scherer−Hodge model (AGSH). These three phenomenological models are most frequently used for the description of experimental structural relaxation data by a suitable set of parameters obtained by curve fitting. The parameter sets reported in the literature for 250 different amorphous material compositions are analyzed on the basis of the isothermal relaxation rate R depending on the nonexponentiality parameter β and the nonlinearity contribution, defined for the TNM, KAHR, and AGSH models as $\sigma = -(\mathrm{d}\ln\tau/\mathrm{d}T_f)_i$. The R_{10} calculated at 10 K below T_g represents a scale for the structural relaxation rate. It describes the structural relaxation kinetics in very different amorphous materials such as organic polymers, epoxy resins, sugars, hydrated starch, simple organic molecules, oxide glasses, chalcogenide glasses, halide glasses, metallic glasses, volcanic glasses, and tektite. This approach can be used for the kinetic comparison of structural relaxation behavior in different amorphous materials as well as in the assessment of the aging treatment and composition design for their future applications.

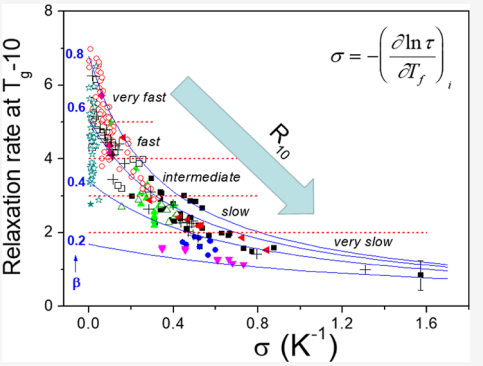

1. INTRODUCTION

The glass transition of the supercooled liquid T_g occurs when the rate of structural rearrangement is similar to the rate of cooling or the duration of an experiment. The gradual approach of volume V, enthalpy H, or other structure-sensitive property to their equilibrium is known as *structural relaxation* or *physical aging*. It has been studied extensively in many noncrystalline materials by various experimental techniques.[1−3] Recent progress is reviewed by several authors in the field of inorganic network glasses,[4] glass-forming polymers,[5] and metallic glasses.[6]

This slow relaxation process[7] has been characterized by the fictive temperature T_f (a parameter representing the liquid structure frozen in the glassy state), introduced by Tool[8,9] in his thermal expansion and density experiments on silicate glasses. Later, Kovacs[10,11] summarized his extensive experimental results of isothermal contraction of organic polymers. These experiments clearly showed that the structural relaxation is nonlinear and nonexponential. Moynihan et al.[12,13] provided a simple method to determine the fictive temperature from differential scanning calorimetry (DSC) data and proposed the stretched exponential response function, ϕ, to account for the nonexponentiality of the relaxation response

$$\phi = \exp(-\xi^{\beta}) \tag{1}$$

where $0 < \beta < 1$ is the non-exponentiality parameter inversely proportional to the width of a corresponding distribution of relaxation times, and ξ is the reduced time defined by Naraynaswamy[14] as

$$\xi = \int_0^t \frac{\mathrm{d}t}{\tau(T,\ T_f)} \tag{2}$$

The relaxation time $\tau(T,T_f)$ depends on both temperature and fictive temperature, and it is defined as

$$\tau(T,\ T_f) = A\cdot \exp\left[x\frac{h^*}{RT} + (1-x)\frac{h^*}{RT_f}\right] \tag{3}$$

where $0 < x \leq 1$ is the nonlinearity parameter. The h^* is the effective activation energy, and A is an adjustable parameter. Equations 1−3 represent the seminal Tool−Narayanaswamy−Moynihan (TNM) phenomenological formalism.[12,13] It is, in fact, identical to the Mazurin, Rekhson, and Startsev approach[15] developed independently for the description of dilatometric structural relaxation data of window glass.

Just a few months later, the essentially equivalent Kovacs−Aklonis−Hutchinson−Ramos (KAHR) phenomenology was developed,[16−18] for the description of structural relaxation in organic polymers. In the KAHR model, a discrete distribution is

Received: January 29, 2023
Revised: March 2, 2023
Published: March 17, 2023

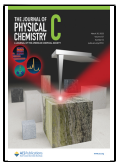

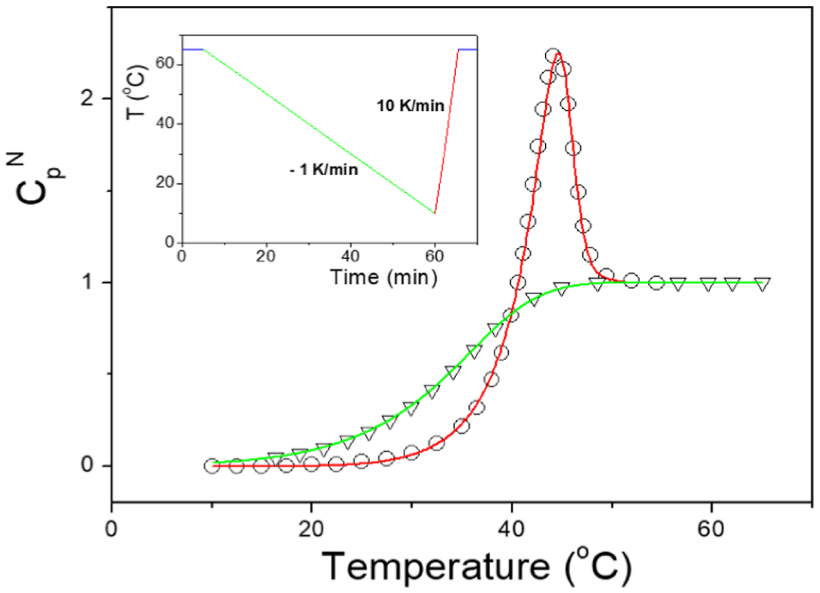

Figure 1. Normalized heat capacity change of selenium in the glass transition range. Points correspond to experimental data[25] for the cooling−heating cycle (indicated in the inset). Solid lines were calculated by the curve fitting procedure using eqs 5 and 6 for the TNM parameters: h^*/R = 42.8 kK, $-\ln(A/s)$ = 133, x = 0.52, β = 0.65.

used, rather than a continuous distribution of relaxation times in the form of the stretched exponential function.[19]

The expression for the relaxation time for the KAHR model is similar to eq 3. Both the TNM and KAHR phenomenology describe the glass transition and structural relaxation quite well. However, there are several shortcomings of this approach. First, eq 3 is empirical, and the parameters ln A, h^*, and x have no clear physical meaning. Second, the prediction of the equilibrium state ($T_f = T$) provides an Arrhenius temperature dependence, which does not agree with the expected Vogel−Fulcher−Tamman (VFT) relation. This may cause somewhat distorted values of ln A and h^*. That problem might reside in an artificial partitioning of the actual and fictive temperature. Despite these shortcomings (rapidly quenched glasses, extremely long aging, etc.), the TNM and KAHR formalisms were successfully applied to describe structural relaxation in many glass-forming systems.[19−21]

It seems that entropy-based theories are more promising, as they provide a natural separation of T and T_f. Based on the Adam−Gibbs[22] cooperative relaxation theory, Scherer[23] and Hodge[24] derived the following expression for the relaxation time

$$\tau(T, T_f) = \tau_0 \exp\left[\frac{Q}{T(1 - T_2/T_f)}\right] \quad (4)$$

where $Q = N_A s^* \Delta\mu / k_B C$. The quantity s^* is the minimum entropy needed for the structural rearrangement, and $\Delta\mu$ is the activation energy for a single rearrangement. In the equilibrium state where $T_f = T$, eq 4 yields the VFT equation with $T_0 = T_2$. Equation 4 in combination with eqs 1 and 2 is referred to here as Adam−Gibbs−Scherer−Hodge (AGSH) phenomenology. The quality of AGSH fits is comparable with that of TNM, although some modest improvements were reported for some organic polymers and inorganic glasses.[20] The main advantage of AGSH probably lies in the physical significance of its parameters.

When the abundant literature related to structural relaxation is inspected, it becomes apparent that the most frequent are calorimetric experiments by DSC, performed particularly in nonisothermal conditions in combination with isothermal aging. Although some correlations of the calculated TNM, KAHR, or AGSH parameters were proposed[20] it is rather uneasy to evaluate their combined effect. On the other hand, isothermal dilatometric experiments provide a suitable basis for such an assessment. Kovacs[10] in his early paper suggested that the inflectional tangent of the contraction isotherm after rapid quenching from T_g, plotted on a logarithmic time scale, could be used as a suitable parameter characterizing the structural relaxation rate.

The aim of this paper is to analyze the structural relaxation behavior for 250 different amorphous material compositions reported in the literature: organic polymers, epoxy resins, sugars, hydrated starch, simple organic molecules, oxide glasses, chalcogenide glasses, halide glasses, metallic glasses, volcanic glasses, and tektite. It is shown that the inflectional tangent of the contraction isotherm taken 10 K below T_g represents a scale for the structural relaxation rate described by the TNM, KAHR, and AGSH parameters. This scale can be used for the kinetic comparison of structural relaxation behavior and aging in different amorphous materials, as well as in the composition design for their future applications.

2. METHODS

2.1. Experimental Data Processing. The typical features of calorimetric glass transition and enthalpy relaxation are illustrated in Figure 1 where the changes of the normalized isobaric heat capacity C_p^N are plotted for pure selenium supercooled liquid and glass (points). The supercooled liquid is after a short isothermal equilibration at 65 °C (5 min) subjected to a downscan to 10 °C by the cooling rate of −1 K/min. The calorimetric liquid-to-glass transition is manifested by the gradual heat capacity drop, corresponding to the relaxation enthalpy lost during cooling. The selenium glass obtained during this defined cooling is then subjected to the subsequent upscan heating at a rate of 10 K/min. The glass-to-liquid transition is characterized by a temperature-shifted heat capacity jump, with a superposed overshoot reflecting the recovery of enthalpy lost during previous cooling (or annealing).

https://doi.org/10.1021/acs.jpcc.3c00637
J. Phys. Chem. C 2023, 127, 6080−6087

The C_p^N sets measured heat capacity (C_p) to zero for the glassy state (C_{pg}) and to unity for supercooled liquid (C_{pl}). DeBolt et al.[13] proposed the analysis of structural relaxation relating the temperature derivative of the fictive temperature (dT_f/dT) and the normalized heat capacity

$$C_p^N = \frac{(C_p - C_{pg})_T}{(C_{pl} - C_{pg})_{T_f}} = \frac{dT_f}{dT} \tag{5}$$

The evolution of the fictive temperature during continuous cooling or heating at a rate $q = dT/dt$ can be expressed by combining eqs 1 and 2 and the Boltzmann superposition principle

$$T_f = T_0 - \sum_{j=1}^{m} \Delta T_j \left\{ 1 - \exp\left[-\left(\sum_{i=1}^{n} \frac{\Delta T_i}{q_i \tau_i} \right)^{\beta} \right] \right\} \tag{6}$$

where T_0 is the initial temperature corresponding to the equilibrium state, i.e., $T_f(T_0) = T_0$ (65 °C for pure selenium). The continuous temperature change is represented by discrete temperature jumps to ensure linearity $\Delta T_i < 0.1$ K.[12,13] The relaxation time τ_i can be expressed by eqs 3 or 4. The parameters of the TNM or AGSH model are then obtained by a curve-fitting procedure by the non-linear optimization method of the temperature-dependent (dT_f/dT) function using the Levenberg−Marquardt algorithm with a minimum of residual sum of squares. The best TNM fits are shown in Figure 1 by full lines for both downscan and upscan thermal treatment. This procedure is usually repeated for different and more complex thermal treatments involving aging.

The typical dilatometric relaxation experiment is illustrated in Figure 2, where the normalized volume contraction ϕ after the down-jump experiment in the selenium glass transition range is plotted as the logarithm of time.

The ϕ sets the volume contraction to unity for unrelaxed glass immediately after the temperature down-jump ($\Delta T = T_0 - T$) and to zero for fully relaxed glass. When $\phi = 0$, the measured volume contraction (ΔV) is equal to the relative departure from extrapolated equilibrium ($\Delta V_{eq} = \Delta\alpha \cdot \Delta T$), where $\Delta\alpha = \alpha_l - \alpha_g$ is the difference of the asymptotic value of the thermal expansion coefficient of equilibrium supercooled liquid and that of glass. The normalized isothermal contraction during isothermal annealing can also be expressed as a function of the fictive temperature T_f

$$\phi = 1 - \left(\frac{\Delta V}{\Delta V_{eq}} \right) = \frac{T_f - T}{\Delta T} \tag{7}$$

The evolution of the fictive temperature during isothermal annealing can be described by dividing the total annealing time into k logarithmically spaced subintervals Δt_k and calculating the corresponding contraction responses at the end of each subinterval. Then, from eqs 1 and 2, and the Boltzmann superposition principle follows

$$T_f = T_0 - \sum_{j=1}^{m} \Delta T_j \left\{ 1 - \exp\left[-\left(\sum_{k=1}^{n} \frac{\Delta t_k}{\tau_k} \right)^{\beta} \right] \right\} \tag{8}$$

The relaxation time τ_i can be expressed by eqs 3 or 4. The parameters of the TNM or AGSH model are then obtained by the curve-fitting procedure by the non-linear optimization method of the time-dependent ϕ function using the Levenberg−Marquardt algorithm with a minimum of the residual sum of squares. The best TNM fit is shown in Figure 2 by the blue solid line for isothermal annealing of selenium after the down-jump from 39 to 32 °C.

2.2. Structural Relaxation Rate. The red line in Figure 2 shows the inflectional tangent $|d\phi/d\log t|_i$ to experimental relaxation data. The isothermal structural relaxation rate at the inflection point can then be expressed as

$$R = \Delta T \left| \frac{d\phi}{d \log t} \right|_i \tag{9}$$

where $\Delta T = T_g - T$. The physical meaning of R is a fictive temperature change per decade of time during the structural relaxation experiment jump at a constant temperature T, taken immediately after a temperature down-jump ΔT. The logarithmic time scale of structural relaxation is inversely proportional to the relaxation rate ($\approx \Delta T/R$). It was shown earlier[26] that R can be expressed for the discussed phenomenological models as

$$R(\Delta T) \cong \left[\frac{1.181}{\beta \Delta T} + \frac{\sigma}{2.303} \right]^{-1} \tag{10}$$

The glass transition temperature T_g is set for the relaxation time $\tau = 100$ s in equilibrium ($T_f = T$). For the TNM model or the KAHR model, then it follows from eq 3: $T_g \approx (h^*/R)/(\ln 100 - \ln A)$. Similarly, for the AGSH model, eq 4 gives: $T_g \approx T_2 + Q/(\ln 100 - \ln \tau_0)$. The parameter σ in eq 10 represents the nonlinearity contribution to the structural relaxation rate at the inflection point and is defined as

$$\sigma = -\left(\frac{\partial \ln \tau}{\partial T_f} \right)_i \tag{11}$$

Taking the first derivative of eq 3 according to eq 11, the parameter σ can be written for the TNM model as[26]

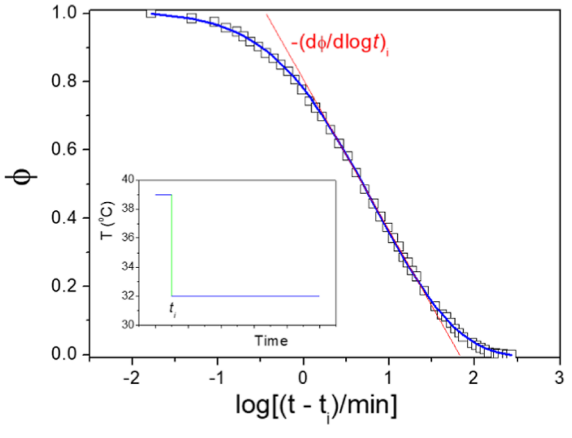

Figure 2. Normalized isothermal volume contraction of selenium in the glass transition range on a logarithmic time scale. Points correspond to dilatometric data[25] for the isothermal annealing after the temperature down-jump experiment (indicated in the inset). The blue solid line was calculated by the curve-fitting procedure using eqs 7 and 8 for the TNM parameters: $h^*/R = 42.8$ kK, $-\ln(A/s) = 133$, $x = 0.42$, $\beta = 0.58$. The red line corresponds to the inflectional tangent $(d\phi/d\log t)_i$.

https://doi.org/10.1021/acs.jpcc.3c00637
J. Phys. Chem. C 2023, 127, 6080−6087

$$\sigma \cong (1 - x)\frac{h^*}{RT_g^{\,2}} \tag{12}$$

and for the KAHR model as

$$\sigma \cong (1 - x)\cdot\theta \tag{13}$$

where $\theta = h^*/RT_g^{\,2}$ is a form of activation energy that ranges from 0.01 to about 1.7 K^{-1} for a wide variety of amorphous materials.[19,20] Similarly, taking the first derivative of eq 4 according to eq 11, the parameter σ can be written for the AGSH model as

$$\sigma \cong \frac{T_2 Q}{T_g(T_g - T_2)^2} \tag{14}$$

3. DISCUSSION

Equation 10 predicts increasing the isothermal relaxation rate R with the magnitude of temperature difference $\Delta T = T_g - T$ strongly depending on both β and σ parameters. The solid lines in Figure 3 show the $R(\Delta T)$ dependences calculated by eqs 10 and 12 for the TNM parameters reported for very slow relaxation of polyvinyl chloride, PVC (β = 0.23, σ = 1.571 K^{-1}),[24] intermediate relaxation of selenium glass, selenium (β = 0.58, σ = 0.257 K^{-1}),[25] and very fast relaxation of As_2S_3 glass (β = 0.82, σ = 0.095 K^{-1}).[26] Open and closed points in Figure 3 correspond to the data reported for dilatometric and calorimetric experiments, respectively. These experimental data agree well within the error margin with the prediction calculated by eq 10. The small deviations for PVC dilatometric data (ΔT > 10 K) are probably caused by an underestimation of R due to a shorter experimental time scale compared to the extremely long relaxation time at equilibrium ($\tau \approx 10^{10}$ s at ΔT = 10 K).

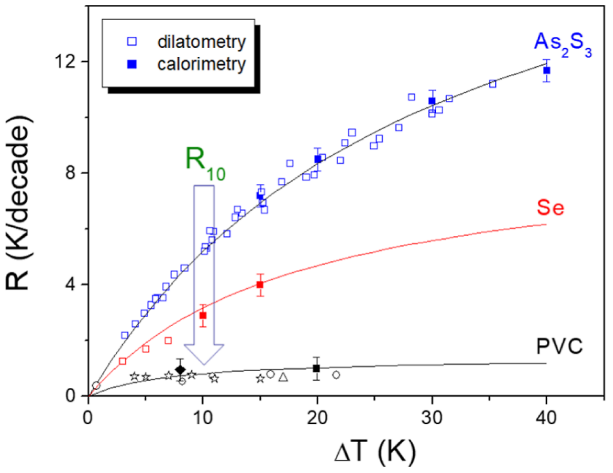

Figure 3. $R(\Delta T)$ dependences for very slow, intermediate, and fast relaxation kinetics. The solid lines were calculated by eqs 10 and 12 for the TNM parameters reported for polyvinyl chloride, PVC (β = 0.23, σ = 1.571 K^{-1}),[24] selenium glass, Se (β = 0.58, σ = 0.257 K^{-1}),[25] and As_2S_3 glass (β = 0.82, σ = 0.095 K^{-1}).[26] Points correspond to experimental data for dilatometric experiments[25−29] (open symbols) and calorimetric experiments[26,30−32] (closed symbols).

It has been shown[26] that, for a structural relaxation rate assessment of different amorphous materials, it is convenient to define the isothermal relaxation rate for a constant ΔT = 10 K, i.e., R_{10} (see Figure 3). In this case, eq 10 can be written as follows

$$R_{10} \cong \left[\frac{0.118}{\beta} + \frac{\sigma}{2.303}\right]^{-1} \tag{15}$$

The R_{10} is in fact the relaxation rate expressed as the fictive temperature change per decade of time during an isothermal structural relaxation experiment taken just 10 K below T_g. Figure 4 shows the R_{10} plotted as a function of the nonlinearity contribution σ. Solid blue lines were calculated by eq 15 for constant values of the nonexponentiality parameter $0.2 \le \beta \le 0.8$. The points correspond to the R_{10} data calculated by eqs 12, 13, and 15 for 250 different sets of TNM and KAHR parameters reported for various types of amorphous materials: polymers,[24,33−43] epoxy resins,[44−51] sugars,[52−55] hydrated starch,[56,57] organic molecules,[58−60] oxide glasses,[13,23,61−69] chalcogenide glasses,[70] halide glasses,[20] metallic glasses,[71,72] volcanic glasses,[73,74] and tektite,[75] as well as for materials described by AGSH parameters.[23−25,45,76−78]

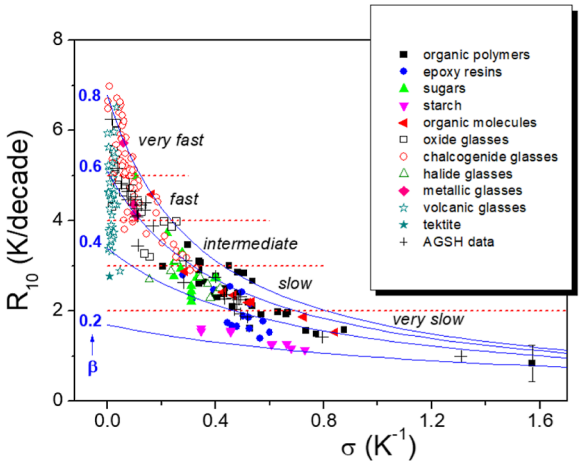

Figure 4. Relaxation rate at T_g −10 as a function of nonlinearity contribution σ. Points correspond to predictions calculated by eqs 12−15 for TNM or KAHR parameters reported for various amorphous materials: organic polymers,[24,33−43] epoxy resins,[44−51] sugars,[52−55] starch,[56,57] organic molecules,[58−60] oxide glasses,[13,23,61−69] chalcogenide glasses,[70] halide glasses,[20] metallic glasses,[71,72] volcanic glasses,[73,74] tektite,[75] and materials described by AGSH parameters.[23−25,45,76−78] Solid lines were calculated by eq 15 for constant values of the nonexponentiality parameter β indicated next to the curves. The dashed lines indicate five different ranges of the structural relaxation rate.

All these data are enclosed within the upper and lower bounds of the nonexponentiality range $0.2 \le \beta \le 0.8$, with notable exception of some chalcogenide glasses such as: $(GeTe_4)_y(GaTe_3)_{100-y}$ and $Ag_x[(GeS_2)_{50}(Sb_2S_3)_{50}]_{100-x}$,[79,80] as well as obsidian volcanic glasses from Tenerife.[74] These materials exhibit very fast structural relaxation characterized by a lower nonlinearity contribution and a high nonexponentiality parameter β > 0.8. In contrast, some organic molecules,[58−60] epoxy resins,[44−51] hydrated starch,[56,57] and vinylic polymers,[24] characterized by considerably higher σ and lower β parameters exhibit a very slow relaxation rate. The upper and lower bounds of the nonexponentiality range (blue solid lines in Figure 4) indicate an available range of the structural relaxation rate at given σ. It is evident that such a range rapidly decreases with σ. Therefore, for amorphous materials with very

https://doi.org/10.1021/acs.jpcc.3c00637
J. Phys. Chem. C 2023, 127, 6080−6087

high nonlinearity contribution (PVC, $\sigma \cong 1.6\ K^{-1}$), the available range of R_{10} is ≈0.4 K/decade of time, which is comparable to the margin of the experimental error. This might explain why it is so difficult to analyze properly very slowly relaxing materials such as PVC[21] or hydrated proteins.[81,82]

The maximum relaxation rate can be expected for $\sigma = 0$ and $\beta = 1$ (exponential relaxation response). From eq 15, it then follows $R_{10}^{max} \cong 8.5$ K/decade. The structural relaxation rate R_{10} of any amorphous material at $T_g - 10$ should be within a scale bounded by this upper limit of the relative change of T_f per decade of time. Therefore, R_{10} can be proposed as a scale to compare the structural relaxation rate of amorphous materials at $T_g - 10$. This relaxation rate scale can be subdivided into five distinct rate ranges (dashed red lines in Figure 4): very fast relaxation $5 < R_{10} < 8.5$, fast relaxation $4 < R_{10} \leq 5$, intermediate relaxation $3 < R_{10} \leq 4$, slow relaxation $2 < R_{10} \leq 3$, and very slow relaxation $R_{10} \leq 2$ K/decade of time. The logarithmic time scale for structural relaxation at $T_g - 10$ is inversely proportional to the relaxation rate ($\approx 10/R_{10}$).

The R_{10} vs σ plot is useful not only for a kinetic comparison of relaxation behavior in different amorphous materials but also for their composition design. It is known that the TNM or AGSH parameters might change for various thermal histories and aging.[20] As these changes likely affect nearly all parameters, it is not as easy to assess their entanglement and complex influence. However, plotting data such as the dependence R_{10} vs σ could help capture the main trends. Some examples are shown in Figure 5. The TNM parameters for hydrated wheat starch

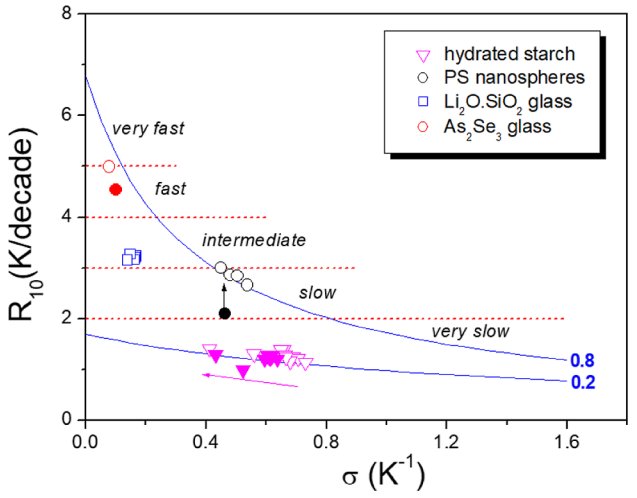

Figure 5. Relaxation rate at $T_g - 10$ as a function of nonlinearity contribution σ. Points correspond to predictions calculated by eqs 12−15 for TNM parameters reported for various thermal histories and aging for amorphous materials: hydrated starch,[57] polystyrene (PS) nanospheres,[40] $Li_2O{\cdot}2SiO_2$ glass,[68] and As_2Se_3 glass.[83,84]

depend on both the aging time and the temperature.[57] Two samples with different levels of hydration (open vs closed triangles) exhibit different values of parameter σ (and slightly different β), resulting in a change in the relaxation rate of these very slowly relaxing systems with aging. Another interesting example is a significant shift in the relaxation rate of polystyrene (PS) nanoparticles[40] under soft and hard confinements. Aqueous, suspended, and silica-capped PS nanoparticles aged under isobaric and isochoric conditions (open circles) relax faster compared to bulk polystyrene (closed circle).[40] In this case, the shift is across almost the entire range for the slow relaxation rate. In contrast, the change in the TNM parameters for $LiO_2{\cdot}2SiO_2$ glasses with various thermal histories and annealing is not significant, and all data points are clustered around $\sigma \approx 0.2$ and $\beta \approx 0.4$, corresponding to the intermediate relaxation rate of this oxide glass.[68] The fast relaxation rate of the As_2Se_3 glass measured by DSC[83] (closed symbol) and dilatometry[84] (open symbol) is shifted, reflecting the increase of the parameter x (0.49 vs 0.57).

Lubchenko and Wolynes[85] extended the random first-order transition (RFOT) theory of the dynamics of supercooled liquid to structural relaxation phenomena below T_g. The theory approximately reproduces the TNM or AGSH phenomenology. The variations of nonexponentiality of relaxation in the glassy state predicted by RFOT theory are rather small in the moderately quenched regime, which seems to be also confirmed experimentally.[57,68] However, the nonlinearity TNM parameter x is shown to be inversely correlated with the fragility index, m. This correlation ($x \cong 19/m$) is like that obtained by AGSH extrapolation, assuming a fixed configurational entropy at T_g.[85] It is also not so different from the experimental findings reported by Böhmer.[86] Combining the correlation proposed by Lubchenko−Wolynes[85] with eq 12 and the Mauro−Yue−Ellison−Gupta−Allan[87] equation for fragility derived from temperature-dependent viscosity data, we can write the following approximation for nonlinearity contribution.

$$\sigma_m \cong \frac{m - 19}{0.434 \cdot T_g} \tag{16}$$

Equation 16 indicates that the nonlinearity contribution of structural relaxation σ_m is proportional to the fragility index and inversely proportional to T_g. It can be estimated from a different type of experimental data. For example, the fragility and T_g values for chalcogenide glass-forming melts can be extracted from a recently reported paper by Koštál et al.,[88] summarizing the viscosity data of these supercooled melts. Fragilities at the glass transition temperature were also determined by viscosity, shear compliance, and modulus measurements for polymers.[89]

Figure 6 shows a comparison of σ values obtained from calorimetric (closed points) or dilatometric (open points)

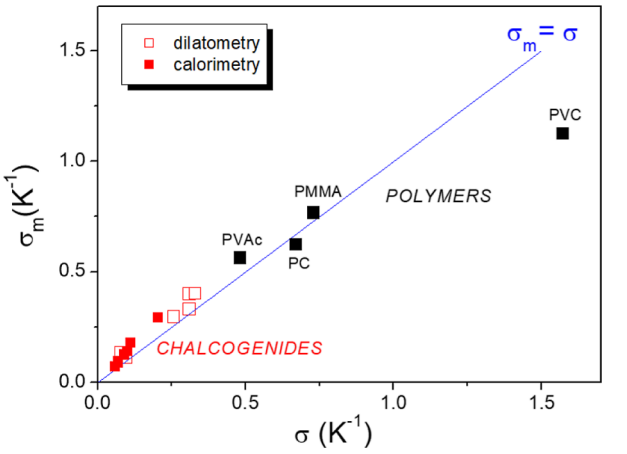

Figure 6. Comparison of parameter σ_m estimated by eq 16 by using viscosity data for chalcogenide melts,[88] viscosity shear compliance, and modulus data for polyvinyl acetate (PVAc), polycarbonate (PC), polymethyl methacrylate (PMMA), and polyvinyl chloride (PVC),[89] and parameter σ calculated by eq 12 using dilatometric and calorimetric structural relaxation data.[70]

https://doi.org/10.1021/acs.jpcc.3c00637
J. Phys. Chem. C 2023, 127, 6080−6087

relaxation data for some chalcogenide glasses and organic polymers calculated in this way by eq 12 along with estimations σ_m obtained by eq 16 for the same materials. It is seen that these estimates based on fragility and T_g value agree reasonably well with the calorimetric or dilatometric structural relaxation experiment. The correlation of the fragility index and the nonexponentiality parameter β was suggested by Böhmer et al.[89] and recently discussed by Doss and Mauro.[90] Therefore, it seems that the structural relaxation rate could probably be controlled mainly by the fragility index and T_g. However, the glass transition temperature might vary because there are different time scales of structural relaxation experiments and viscosity or shear compliance measurements.

The relaxation rate scale discussed here is a useful tool for comparing various glass-forming systems subjected to different thermal treatments and aging. Nevertheless, it is based on the implicit assumption of a single fictive temperature. The RFOT theory suggests that no glass can accurately be described by a single global fictive temperature.[85] Over the past decade, considerable progress has been made deeper into the energy landscape, especially in a regime of ultrastable, low-energy glasses. Ediger et al.,[91] in a recently published perspective, point out that the glassy state seems to be rather heterogeneous in terms of local fictive temperature where the degree of local inhomogeneity depends on the preparation and aging history. On the other hand, the classical single fictive temperature TNM model is very useful for quench rate estimations of volcanic glasses.[73] This "geospeedometric" approach can be used in a variety of situations where the melt cannot be measured during eruption and can provide independent testing in cases where volcanic melts can be evaluated experimentally.[74] The classical TNM model has also been used to predict the final size, shape, refraction index,[64,65] or elastic modulus[92] of precisely molded oxide glass optical lenses. The environmental and economic impact of the ultra-precision thermoforming of all classes of glass optical elements has considerable advantages over classical grinding and polishing.[93] Therefore, the structural relaxation rate estimation during thermoforming of amorphous optical materials is of great practical importance.

4. CONCLUSIONS

In summary, we have shown that the isothermal structural relaxation rate R depends on ΔT, the nonexponentiality parameter β, and the nonlinearity contribution σ. A simple equation connecting R and these variables was derived for the TNM, KAHR, and AGSH models. This equation has been tested for three amorphous materials that exhibit different relaxation rates. The prediction agrees well with the calorimetric and dilatometric experimental data within the experimental error margin. We have shown that R_{10} calculated at 10 K below T_g defines a scale that describes structural relaxation kinetics in very different amorphous materials such as organic polymers, epoxy resins, sugars, hydrated starch, simple organic molecules, oxide glasses, chalcogenide glasses, halide glasses, metallic glasses, volcanic glasses, and tektite. This relaxation rate scale can be used for the kinetic comparison of structural relaxation behavior and aging in different amorphous materials, as well as in composition design for their future applications.

AUTHOR INFORMATION

Corresponding Author

Jiří Málek − *Department of Physical Chemistry, Faculty of Chemical Technology, University of Pardubice, Pardubice 532 10, Czech Republic;* orcid.org/0000-0002-7502-5320; Email: jiri.malek@upce.cz

Complete contact information is available at: https://pubs.acs.org/10.1021/acs.jpcc.3c00637

Notes

The author declares no competing financial interest.

ACKNOWLEDGMENTS

This work was supported by the Selected Research Teams Program of the Faculty of Chemical Technology, University of Pardubice.

REFERENCES

(1) Zheng, Q.; Zhang, Y.; Montazerian, M.; Gulbiten, O.; Mauro, J. C.; Zanotto, E. D.; Yue, Y. Understanding Glass through Differential Scanning Calorimetry. *Chem. Rev.* **2019**, *119*, 7848−7939.
(2) Richert, R.; Gabriel, J. P.; Thoms, E. Structural Relaxation and Recovery: A Dielectric Approach. *J. Phys. Chem. Lett.* **2021**, *12*, 8465−8469.
(3) Bennin, T.; Xing, E.; Ricci, J.; Ediger, M. D. Rejuvenation Versus Overaging: The Effect of Cyclic Loading/Unloading on the Segmental Dynamics of Poly(methyl methacrylate) Glasses. *Macromolecules* **2020**, *53*, 8467−8475.
(4) Micoulaut, M. Relaxation and Physical Aging in Network Glasses: A Review. *Rep. Prog. Phys.* **2016**, *79*, 066504.
(5) McKenna, G. B.; Simon, S. L. 50th Anniversary Perspective: Challenges in the Dynamics and Kinetics of Glass-Forming Polymers. *Macromolecules* **2017**, *50*, 6333−6361.
(6) Wang, W. H. Dynamic Relaxations and Relaxation-Property Relationships in Metallic Glasses. *Prog. Mater. Sci.* **2019**, *106*, 100561.
(7) Hodge, I. M. Physical Aging in Polymer Glasses. *Science* **1995**, *267*, 1945−1947.
(8) Tool, A. Q. Relation between Inelastic Deformability and Thermal Expansion of Glass in Its Annealing Range. *J. Am. Ceram. Soc.* **1946**, *29*, 240−253.
(9) Tool, A. Q. Effect of Heat-treatment on the Density and Constitution of High-silica Glasses of the Borosilicate Type. *J. Am. Ceram. Soc.* **1948**, *31*, 177−186.
(10) Kovacs, A. J. La contraction isotherme du volume des polymeres amorphes. *J. Polym. Sci.* **1958**, *30*, 131−147.
(11) Kovacs, A. J. Transition vitreuse dans les polymeres amorphes. Etude phénoménologique. *Fortschr. Hochpolym.-Forsch.* **1963**, *3*, 394−507.
(12) Moynihan, C. T.; Easteal, A. J.; DeBolt, M. A.; Tucker, J. Dependence of the Fictive Temperature of Glass on Cooling Rate. *J. Am. Ceram. Soc.* **1976**, *59*, 12−16.
(13) DeBolt, M. A.; Easteal, A. J.; Macedo, P. B.; Moynihan, C. T. Analysis of Structural Relaxation in Glass Using Rate Heating Data. *J. Am. Ceram. Soc.* **1976**, *59*, 16−21.
(14) Narayanaswamy, O. S. A Model of Structural Relaxation in Glass. *J. Am. Ceram. Soc.* **1971**, *54*, 491−498.
(15) Mazurin, O. V.; Rekhson, S. M.; Startsev, Y. K. The Role of Viscosity in the Calculation of the Properties of Glass in the Glass-Transition Region. *Fiz. Khim. Stekla* **1975**, *1*, 412−416. (English translation)
(16) Hutchinson, J. M.; Aklonis, J. J.; Kovacs, A. J. New Phenomenological Approach to Volume Recovery in Glasses. *Am. Chem. Soc.* **1975**, *170*, 21.
(17) Hutchinson, J. M.; Kovacs, A. J. A Simple Phenomenological Approach to the Thermal Behavior of Glasses During Uniform Heating or Cooling. *J. Polym. Sci., Polym. Phys. Ed.* **1976**, *14*, 1575−1590.
(18) Kovacs, A. J.; Aklonis, J. J.; Hutchinson, J. M.; Ramos, A. R. Isobaric Volume and Enthalpy Recovery of Glasses. II. A Transparent Multiparameter Theory. *J. Polym. Sci., Polym. Phys. Ed.* **1979**, *17*, 1097−1162.

(19) Hutchinson, J. M. Physical Aging in Polymers. *Prog. Polym. Sci.* **1995**, *20*, 703−760.
(20) Hodge, I. M. Enthalpy Relaxation and Recovery in Amorphous Materials. *J. Non-Cryst. Solids* **1994**, *169*, 211−266.
(21) Hodge, I. M. A Personal Account of Developments in Enthalpy Relaxation: A Tribute to C.T. Moynihan. *J. Am. Ceram. Soc.* **2008**, *91*, 766−772.
(22) Adam, G.; Gibbs, J. H. On the Temperature Dependence of Cooperative Relaxation Properties in Glass-Forming Liquids. *J. Chem. Phys.* **1965**, *43*, 139−146.
(23) Scherer, G. W. Volume Relaxation Far from Equilibrium. *J. Am. Ceram. Soc.* **1986**, *69*, 374−381.
(24) Hodge, I. M. Effects of Annealing and Prior History on Enthalpy Relaxation in Glassy Polymers.6. Adam-Gibbs Formulation of Nonlinearity. *Macromolecules* **1987**, *20*, 2897−2908.
(25) Málek, J.; Svoboda, R.; Pustková, P.; Čičmanec, P. Volume and Enthalpy Relaxation of a-Se in the Glass Transition Region. *J. Non-Cryst. Solids* **2009**, *355*, 264−272.
(26) Málek, J. Volume and Enthalpy Relaxation Rate in Glassy Materials. *Macromolecules* **1998**, *31*, 8312−8322 and references quoted in.
(27) Greiner, R.; Schwarzl, F. R. Thermal Contraction and Volume Relaxation of Amorphous Materials. *Rheol. Acta* **1984**, *23*, 378−395.
(28) Struik, L. C. E. Volume Relaxation and Secondary Transitions in Amorphous Polymers. *Polymer* **1987**, *28*, 1869−1875.
(29) Lee, H. H. D.; Mc Garry, F. J. Changes in Free-Volume and Mechanical Properties of PVC Films Incurred by Quenching and Aging. *J. Macromol. Sci. Phys.* **1990**, *29*, 11−29.
(30) Zhao, H. Y.; Koh, Y. P.; Pyda, M.; Sen, S.; Simon, S. L. The Kinetics of the Glass Transition and Physical Aging in Germanium Selenide Glasses. *J. Non-Cryst. Solids* **2013**, *368*, 63−70.
(31) Pappin, A. J.; Hutchinson, J. M.; Ingram, M. D. Enthalpy Relaxation in Polymer Glasses − Evaluation and Interpretation of the Tool-Narynaswamy Parameter-x for Poly(vinyl chloride). *Macromolecules* **1992**, *25*, 1084−1089.
(32) Ribelles, J. L. G.; Diaz-Calleja, R.; Ferguson, R.; Cowie, J. M. G. Glass-Transition and Physical Aging in Plasticized Poly(vinyl chloride). *Polymer* **1987**, *28*, 2262−2266.
(33) Hodge, I. M.; Huvard, G. S. Efects of Annealing and Prior History on Enthalpy Relaxation in Glassy Polymers. 3. Experimental and Modeling Studies on Polystyrene. *Macromolecules* **1983**, *16*, 371−375.
(34) Badrinarayanan, P.; Simon, S. L.; Lyng, R. J.; O'Reilly, J. M. Effect of Structure on Enthalpy Relaxation of Polycarbonate: Experiments and Modelling. *Polymer* **2008**, *49*, 3554−3560.
(35) Hodge, I. M. Effects of annealing and prior history on enthalpy relaxation in glassy polymers. 4. Comparison of five polymers. *Macromolecules* **1983**, *16*, 898−902.
(36) Svoboda, R.; Pustková, P.; Málek, J. Structural Relaxation of Polyvinyl Acetate (PVAc). *Polymer* **2008**, *49*, 3176−3185.
(37) O'Reilly, J. M. Physical Aging and Enthalpy Relaxation of Amorphous Polyesters. *J. Polym. Sci., Part B: Polym. Phys.* **2000**, *38*, 495−499.
(38) Sasabe, H.; Moynihan, C. T. Structural Relaxation in Poly (vinyl acetate). *J. Polym. Sci., Polym. Phys. Ed.* **1978**, *16*, 1447−1457.
(39) Aou, K.; Hsu, S. L.; Kleiner, L. W.; Tang, F. W. Roles of Conformational and Configurational Defects on the Physical Aging of Amorphous Poly(lactic acid). *J. Phys. Chem. B* **2007**, *111*, 12322.
(40) Guo, Y.; Zhang, C.; Lai, C.; Priestley, R. D.; D'Acunzi, M.; Fytas, G. Structural Relaxation of Polymer Nanospheres under Soft and Hard Confinement: Isobaric versus Isochoric Conditions. *ACS Nano* **2011**, *5*, 5365−5373.
(41) Koh, Y. P.; Simon, S. L. Enthalpy Recovery of Polystyrene: Does a Long-Term Aging Plateau Exist? *Macromolecules* **2013**, *46*, 5815−5821.
(42) Li, Q.; Simon, S. L. Enthalpy Recovery of Polymeric Glasses: Is the Theoretical Limiting Liquid Line Reached? *Polymer* **2006**, *47*, 4781−4788.
(43) Liu, G.; Li, L.; Zheng, Y.; Zuo, Y. Temperature Gradient in Sample and its Effect on Enthalpy Relaxation Model Fitting of Polystyrene. *J. Non-Cryst. Solids* **2013**, *365*, 13−22.
(44) Montserrat, S.; Calventus, Y.; Hutchinson, J. M. Physical Aging of Thermosetting Powder Coatings. *Prog. Org. Coating* **2006**, *55*, 35−42.
(45) Hutchinson, J. M.; McCarthy, D.; Montserrat, S.; Cortes, P. Enthalpy Relaxation in Partially Cured Epoxy Resin. *J. Polym. Sci., Part B: Polym. Phys.* **1996**, *34*, 229−239.
(46) Montserrat, S.; Cortés, P.; Pappin, A. J.; Quah, K. H.; Hutchinson, J. M. Structural Relaxation in Fully Cured Epoxy Resins. *J. Non-Cryst. Solids* **1994**, *172*−*174*, 1017−1022.
(47) Cortés, P.; Montserrat, S.; Hutchinson, J. M. Addition of a Reactive Diluent to a Catalyzed Epoxy-Anhydride System. II. Effect on Enthalpy Relaxation. *J. Appl. Polym. Sci.* **1997**, *63*, 17−25.
(48) Montserrat, S.; Cortes, P.; Calventus, Y.; Hutchinson, J. M. Effect of Crosslink Length on the Enthalpy Relaxation of Fully Cured Epoxy-Diamine Resins. *J. Polym. Sci., Polym. Phys. Ed.* **2000**, *38*, 456−468.
(49) Ramírez, C.; Abad, M. J.; Cano, J.; López, J.; Nogueira, P.; Barral, L. Enthalpy Relaxation in an Epoxy-Cycloaliphatic Amine Resin. *Colloid Polym. Sci.* **2001**, *279*, 184−189.
(50) Morancho, J. M.; Salla, J. M. Relaxation in a Neat Epoxy Resin and in the Same Resin Modified with a Carboxyl-Terminated Copolymer. *J. Non-Cryst. Solids* **1998**, *235*−*237*, 596−599.
(51) Lu, H.; Nutt, S. Enthalpy Relaxation of Layered Silicate-Epoxy Nanocomposites. *Macromol. Chem. Phys.* **2003**, *204*, 1832−1841.
(52) Wungtanagorn, R.; Schmidt, S. J. Phenomenological Study of Enthalpy Relaxation of Amorphous Glucose, Fructose and their Mixture. *Thermochim. Acta* **2001**, *369*, 95−116.
(53) Gao, C.; Ye, B.; Jiang, B.; Liu, X. N. Comparative Investigation on the Enthalpy Relaxation of Four Amorphous Pentose Isomers. *J. Therm. Anal. Calorim.* **2014**, *115*, 37−44.
(54) Gao, C.; Ma, H. M. Enthalpy Relaxation in D-Sorbitol Glass. *J. Therm. Anal. Calorim.* **2015**, *120*, 1905−1912.
(55) Hill, S. A.; MacNaughtan, W.; Farhat, I. A.; Noel, T. R.; Parker, R.; Ring, S. G.; Whitcombe, M. J. The Effect of Thermal History on the Maillard Reaction in a Glassy Matrix. *J. Agric. Food Chem.* **2005**, *53*, 10213−10218.
(56) Noel, T. R.; Parker, R.; Brownsey, G. J.; Farhat, I. A.; MacNaughtan, W.; Ring, S. G. Physical Aging of Starch, Maltodextrin, and Maltose. *J. Agric. Food Chem.* **2005**, *53*, 8580−8585.
(57) Morris, C.; Taylor, A. J.; Farhat, I. A.; MacNaughtan, W. Modelling of Physical Ageing in Starch using the TNM Equation. *Carbohydr. Res.* **2011**, *346*, 1122−1128.
(58) Hodge, I. M.; O'Reilly, J. M. Nonlinear Kinetic and Thermodynamic Properties of Monomeric Organic Glasses. *J. Phys. Chem. B* **1999**, *103*, 4171−4176.
(59) Sartor, G.; Johari, G. P. Structural Relaxation and Calorimetry in the Glass-Softening Range of 1,3,5-Tris(1-naphtyl) benzene. *J. Phys. Chem. B* **1999**, *103*, 11036−11040.
(60) Moynihan, C. T.; Crichton, S. N.; Opalka, S. M. Linear and Non-Linear Structural Relaxation. *J. Non-Cryst. Solids* **1991**, *131*−*133*, 420−434.
(61) Scherer, G. W. Use of the Adam-Gibbs Equation in the Analysis of Structural Relaxation. *J. Am. Ceram. Soc.* **1984**, *67*, 504−511.
(62) Crichton, S. N.; Moynihan, C. T. Structural Relaxation of Lead Silicate Glass. *J. Non-Cryst. Solids* **1988**, *102*, 222−227.
(63) Moynihan, C. T.; Easteal, A. J.; Tran, D. C.; Wilder, J. A.; Donovan, E. P. Heat-Capacity and Structural Relaxation of Mixed-Alkali Glasses. *J. Am. Ceram. Soc.* **1976**, *59*, 137−140.
(64) Gaylord, S.; Ananthasayanam, B.; Tincher, B.; Petit, L.; Cox, C.; Fotheringham, U.; Joseph, P.; Richardson, K. Thermal and Structural Property Characterization of Commercially Moldable Glasses. *J. Am. Ceram. Soc.* **2010**, *93*, 2207−2214.
(65) Fotheringham, U.; Baltes, A.; Fischer, P.; Höhn, P.; Jedamzik, R.; Schenk, C.; Stolz, C.; Westenberger, G. Refractive Index Drop Observed After Precision Molding of Optical Elements: Quantitative Understanding Based on the Tool-Naraynaswamy-Moynihan Model. *J. Am. Ceram. Soc.* **2008**, *91*, 780−783.

https://doi.org/10.1021/acs.jpcc.3c00637
J. Phys. Chem. C 2023, 127, 6080−6087

(66) Zhu, X.; Shu, C.; Zheng, Q.; Yin, S. Numerical Simulation of the Structural Relaxation Characteristics of K-LCV161 Glass. *J. Non-Cryst. Solids* **2021**, *571*, 121050.
(67) Chromčíková, M.; Hruška, B.; Nowicka, A.; Svoboda, R.; Liška, M. Structural Relaxation and Viscosity of Al_2O_3 Doped Magnesium Phosphate Glasses. *J. Non-Cryst. Solids* **2020**, *550*, 120323.
(68) Han, Y.; D'Amore, A.; Marino, G.; Nicolais, L. A Phenomenological Study of the Structural Relaxation of an Inorganic Glass ($Li_2O.2SiO_2$). *Mater. Chem. Phys.* **1998**, *55*, 155−159.
(69) Han, Y.; D'amore, A.; Nicolais, L. Analysis of Structural Relaxation in a $Li_2O.2SiO_2$ Glass using Rate Heating Approach. *J. Mater. Sci.* **1999**, *34*, 1899−1904.
(70) Málek, J. Structural Relaxation in Chalcogenide Glasses. *J. Am. Ceram. Soc.* **2023**, *106*, 1739−1747 and references quoted in.
(71) Wang, T.; Yang, Y. Q.; Li, J. B.; Rao, G. H. Thermodynamics and Structural Relaxation in Ce-Based Bulk Metallic Glass-Forming Liquid. *J. Alloys Compd.* **2011**, *509*, 4569−4573.
(72) Martin, S. W.; Walleser, J.; Karthikeyan, D.; Sordelet, D. Enthalpy Relaxation Studies of the Glass Transition in a Metallic Glass. *J. Non-Cryst. Solids* **2004**, *349*, 347−354.
(73) Wilding, M.; Webb, S.; Dingwell, D. B. Evaluation of a Relaxation Geospeedometer for Volcanic Glasses. *Chem. Geol.* **1995**, *125*, 137−148.
(74) Wilding, M.; Webb, S.; Dingwell, D. B.; Ablay, G.; Marti, J. Cooling Rate Variation in Natural Volcanic Glasses from Tenerife, Canary Islands. *Contrib. Mineral. Petrol.* **1996**, *125*, 151−160.
(75) Wilding, M.; Webb, S.; Dingwell, D. B. Tektite Cooling Rates: Calorimetric Relaxation Geospeedometry Applied to a Natural Glass. *Geochim. Cosmochim. Acta* **1996**, *60*, 1099−1103.
(76) Andreozzi, L.; Faetti, M.; Giordano, M.; Palazzuoli, D.; Zulli, F. Enthalpy Relaxation in Polymers: A Comparison among Different Multiparameter Approaches Extending the TNM/AGV Model. *Macromolecules* **2003**, *36*, 7379−7387.
(77) Hodge, I. M. Adam-Gibbs Formulation of Non-Linear Enthalpy Relaxation. *J. Non-Cryst. Solids* **1991**, *131*−*133*, 435−441.
(78) Sales, B. C. Structural Relaxation Dynamics of Phosphate Glasses: The Effects of Network Topology on the Glass Transition. *J. Non-Cryst. Solids* **1990**, *119*, 136−150.
(79) Svoboda, R.; Setnička, M.; Zmrhalová, Z.; Brandová, D.; Málek, J. Structural Interpretation of the Enthalpy Relaxation Kinetics of $(GeTe_4)_y(GaTe_3)_{1-y}$ Far-Infrared Glasses. *J. Non-Cryst. Solids* **2016**, *447*, 110−116.
(80) Svoboda, R.; Fraenkl, M.; Frumarová, B.; Wágner, T.; Málek, J. Thermokinetic Behaviour of Ag-Doped $(GeS_2)_{50}(Sb_2S_3)_{50}$ Glasses. *J. Non-Cryst. Solids* **2016**, *449*, 12−19.
(81) Sartor, G.; Mayer, E.; Johari, G. P. Calorimetric Studies of the Kinetic Unfreezing of Molecular Motions in Hydrated Lysozyme, Hemoglobin and Myoglobin. *Biophys. J.* **1994**, *66*, 249−258.
(82) Hodge, J. M. Application of the Thermorheologically Complex Nonlinear Adam-Gibbs Model for the Glass Transition to Molecular Motion in Hydrated Proteins. *Biophys. J.* **2006**, *91*, 993−995.
(83) Easteal, A. J.; Wilder, J. A.; Mohr, R. K.; Moynihan, C. T. Heat Capacity and Structural Relaxation of Enthalpy in As_2Se_3 Glass. *J. Am. Ceram. Soc.* **1977**, *60*, 134−138.
(84) Málek, J.; Shánělová, J. Structural Relaxation of As_2Se_3 Glass and Viscosity of Supercooled Liquid. *J. Non-Cryst. Solids* **2005**, *351*, 3458−3467.
(85) Lubchenko, V.; Wolynes, P. G. Theory of Aging in Structural Glasses. *J. Chem. Phys.* **2004**, *121*, 2852−2865.
(86) Böhmer, R. Non-Linearity and Non-Exponentiality of Primary Relaxations. *J. Non-Cryst. Solids* **1994**, *172*−*174*, 628−634.
(87) Mauro, J. C.; Yue, Y.; Ellison, A. J.; Gupta, P. K.; Allan, D. C. Viscosity of Glass-Forming Liquids. *Proc. Natl. Acad. Sci. U.S.A.* **2009**, *106*, 19780−19784.
(88) Koštál, P.; Shánělová, J. J.; Málek, J. Viscosity of Chalcogenide Glass-Formers. *Int. Mater. Rev.* **2020**, *65*, 63−101.
(89) Böhmer, R.; Ngai, K. L.; Angell, C. A.; Plazek, D. J. Nonexponential Relaxations in Strong and Fragile Glass Formers. *J. Chem. Phys.* **1993**, *99*, 4201−4209.
(90) Doss, K.; Mauro, J. C. Impact of Dynamic Stretching Exponent on the Correlation between Liquid Fragility and Nonexponentiality at the Glass Transition. *J. Phys.: Condens. Matter* **2022**, *34*, 455402.
(91) Ediger, M. D.; Gruebele, M.; Lubchenko, V.; Wolynes, P. G. Glass Dynamics Deep in the Energy Landscape. *J. Phys. Chem. B* **2021**, *125*, 9052−9068.
(92) Liu, W.; Ruan, H.; Zhang, L. Revealing Structural Relaxation of Optical Glass Through the Temperature Dependence of Young's Modulus. *J. Am. Ceram. Soc.* **2014**, *97*, 3475−3482.
(93) Schaub, M.; Schwiegerling, J.; Fest, E.; Shepard, R. H.; Symmons, A. *Molded Optics: Design and Manufacture*; CRC Press: New York, 2011.

https://doi.org/10.1021/acs.jpcc.3c00637
J. Phys. Chem. C 2023, 127, 6080−6087